# Characteristics and Potential Values of Bio-Products Derived from Switchgrass Grown in a Saline Soil Using a Fixed-Bed Slow Pyrolysis System

Yan Yue,[a] Qimei Lin,[a,]* Muhammad Irfan,[a] Qun Chen,[b] Xiaorong Zhao,[a] and Guitong Li [a]

Switchgrass harvested from saline soil was slowly pyrolyzed at 300, 500, and 700 °C in a fixed-bed reactor. The objective was to understand the characteristics and evaluate the potential values of the bio-oil, syngas, and biochar. The biochar yield (27.0% to 41.3%) decreased with increasing temperature, whereas the syngas yield (26.3% to 40.9%) increased. The bio-oil yield (30.8% to 34.1%) was highest when the switchgrass was pyrolyzed at 500 °C. Both the bio-oil and syngas had low value as direct fuels because of their low heating values. Compared with the biochars from the switchgrass grown in "sweet" soil, the biochars derived from the switchgrass grown in saline soil had higher values of ash (10.5% to 17.2%), mineral nutrients, and cation exchange capacity (CEC) (200.3 to 241.1 cmol/kg). These results suggested that the biochar generated in this study might have a better liming effect and improvement of soil fertility and crop growth as a soil conditioner, and lead to double wins in saline soil improvement and a new approach for switchgrass utilization.

*Keywords: Switchgrass; Slow pyrolysis; Bio-oil; Syngas; Biochar*

*Contact information: a: Department of Soil and Water Science, College of Resources and Environment, China Agricultural University, Beijing 100193, China; b: Key Laboratory for Thermal Science and Power Engineering of Ministry of Education, Department of Thermal Engineering, Tsinghua University, Beijing 100084, China; *Corresponding author: linqm@cau.edu.cn*

## INTRODUCTION

Pyrolysis is an effective method for the high-efficiency utilization of biomass resources. The products generated vary with the pyrolysis conditions and processes (Kan *et al.* 2016). The main bio-products from slow pyrolysis are biochar, syngas, and bio-oil. Syngas and bio-oil can be directly used as fuels and chemical materials (Chen *et al.* 2016). Biochar can be used as a soil conditioner and a fuel and adsorption material (Tsai *et al.* 2012; Kan *et al.* 2016; Kuppusamy *et al.* 2016). Emerging data have shown that biochar used as soil amendment remarkably influences the physical, chemical, and microbiological properties of the soil. These influences include reducing soil bulk density, improving soil porosity and aggregation, increasing water holding capacity and water availability (Nelissen *et al.* 2015; Zhang *et al.* 2016), increasing soil pH, decreasing the toxicity of $Al^{3+}$ and $Mn^{2+}$ in acidic soil, enhancing the soil cation exchange capacity (CEC), increasing nutrient availability and nutrient use efficiency (Dong *et al.* 2013; Yuan *et al.* 2016), increasing gram negative bacteria ($G^-$) and actinomycetes abundance, and reducing gram positive bacteria ($G^+$) abundance (Luo 2012). Both field and pot trials in tropical, subtropical, and temperate zones have shown that biochar soil amendment induces major increases in the crop yields of cereals, legumes, and tubers (Biederman and Harpole 2013). Furthermore, an increasing amount of data shows that biochar amendment has a high potential value for reducing greenhouse gas emissions, sequestrating carbon (Zhang *et al.*

2016), denaturing heavy metals, and stimulating the decomposition of organic pollutants (Chen *et al.* 2015).

Switchgrass (*Panicum virgatum*) can be used for forage, landscape conservation, as a potential bio-energy crop to generate power by combustion, and to produce ethanol or biodiesel by pyrolysis (Jiang *et al.* 2014). It is resistant to salt and alkali and drought, and it can grow in saline soil and regions that are arid and semiarid. Approximately 9150 $hm^2$ of saline and sodic soils in northern China are suitable to grow switchgrass. The biomass production can reach up to 10 $t/hm^2$ in the saline and sodic soils in the Hetao region of Inner Mongolia, China (Huang 2017). With consideration of the profits of both biochar soil amendment and saline soil utilization, it may show some advantages and economical values to grow switchgrass in inland saline and sodic soils, and then process the produced biomass with slow pyrolysis.

In this study, switchgrass biomass, collected from saline soil in the Hetao region, was pyrolyzed at 300, 500, and 700 °C in a fixed-bed slow pyrolysis system, and the characteristics of the bio-oil, syngas, and biochar were analyzed. The objectives of this study were: (1) to understand the composition of the bio-oil and syngas produced at different pyrolysis temperatures and evaluate their energy values; (2) to characterize the biochar produced at different pyrolysis temperatures and evaluate the potential value as a soil conditioner; and (3) to determine the optimal temperature for processing switchgrass grown in saline soil with a fixed-bed slow pyrolysis system.

## EXPERIMENTAL

### Switchgrass

Switchgrass was planted in a sulfate saline soil in the Hetao region of Inner Mongolia, China in 2012. The amount of above-ground dry matter was 7.34 $t/hm^2$ in 2013, which contained 31.55% hemicellulose, 40.43% cellulose, 9.98% lignin, 5.47% ash, and 12.57% other extractives. The contents of C, H, N, mineral nutrients, and water-soluble ions are shown in Table 1.

### Pyrolysis Device

Biochar, syngas, and bio-oil are produced in a fixed-bed biomass pyrolysis system, as shown in Fig. 1. The system consisted of a pyrolysis reactor, bio-oil collector, syngas discharge pipe, condensing system, thermal controller, and data logger. The pyrolysis reactor was composed of an electric heater and a stainless steel reactor. Five thermocouples were used to monitor the temperature along the height of the reactor. The data of temperature were recorded by a data logger. At the top of the reactor, an insulated stainless steel pipe was used to connect the pyrolysis reactor with a vertical fixed-condenser (a shell-and-tube heat exchanger). The coolant flowed out of the condenser from the top and circulated back to the pump. At the exit of the condenser, a bio-oil trap was attached to collect the condensed bio-oil. The exit of the bio-oil trap was connected with a tube for gas sampling and exhaust. The volatile vapors and low molecular weight gases were cooled down to temperature near 0 °C. The condensable gases were condensed to form bio-oil and collected in the bio-oil trap. Non-condensing gases exited the trap to the sampling and exhaust pipe.

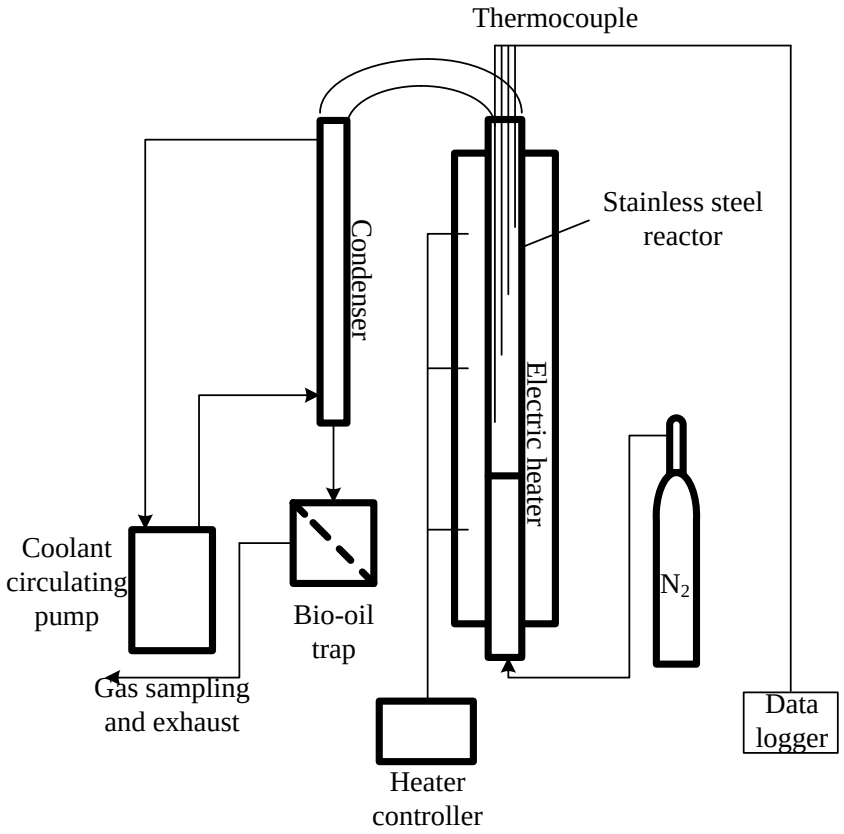


**Fig. 1.** Schematic diagram of the biomass pyrolysis system

## Pyrolysis

One hundred grams of air-dried switchgrass (2- to 3-cm fragments) were placed into the pyrolysis reactor. The data logger was turned on, and the heating program was started with a heating rate of 10 °C/min and a flowing $N_2$ atmosphere of 1 L/min. The pyrolysis reaction was maintained for 2 h when the temperature reached to 300, 500, and 700 °C, respectively. One liter of gas was sampled every 30 min at set temperatures with air sampling bags. The mixed syngas samples were marked as G300, G500, and G700 for the switchgrass pyrolyzed at 300, 500, and 700 °C, respectively, and were measured by a gas chromatograph (Perkin Elmer AutoSystem XL, Waltham, MA, USA). The lower heating value (LHV) was calculated from the measured gases. The LHV of the syngas was calculated according to the following equation (Kan *et al.* 2016),

$$LHV\ (\mathrm{MJ/Nm^3}) = (107.98 \times \psi H_2 + 126.36 \times \psi CO + 358.18 \times \psi CH_4 + 59.04 \times \psi C_2H_4 + 63.77 \times \psi C_2H_6 + 93.03 \times \psi C_3H_8 + 56.36 \times \psi C_2H_2) / 1000 \quad (1)$$

where $\psi$ refers to the volume percentages of the measured gases. The biochars were marked as B300, B500, and B700, and the bio-oils collected by a bio-oil trap were marked as O300, O500, and O700 for the switchgrass pyrolyzed at 300, 500, and 700 °C, respectively. The products were collected after cooling down to room temperature at the end of the pyrolysis reaction. The products were then measured for their masses and compositions, and the physical and chemical characteristics were analyzed.

**Table 1.** Chemical Properties of the Biochar Derived from Switchgrass Pyrolyzed in a Fixed-Bed Pyrolysis System

| Feedstock/ biochars | C | H | O | N | Ash | H/C | O/C | pH | EC[1] | WSOC[2] | WSN[3] | WSP[4] | $K^+$ | $Na^+$ | $Ca^{2+}$ | $Mg^{2+}$ |
|---|---|---|---|---|---|---|---|---|---|---|---|---|---|---|---|---|
| | % | | | | | | | | (mS/cm) | (g/kg) | | | | | | |
| Feedstock | 45.50d | 5.83a | 42.59a | 0.61a | 5.47c | 1.54a | 0.70a | 5.67d | 2.04b | 6.41a | 0.17a | 0.51a | 4.74c | 0.19b | 0.65a | 6.48a |
| B300 | 63.41c | 4.10b | 21.38b | 0.65a | 10.46b | 0.78b | 0.25b | 6.96c | 0.98d | 0.44b | 0.04b | 0.04b | 1.79d | 0.06d | 0.25a | 1.98b |
| B500 | 71.67b | 2.19c | 8.67c | 0.63a | 16.84a | 0.37c | 0.09c | 9.75b | 1.98c | 0.32b | 0.04b | 0.02c | 5.72b | 0.15c | 0.19a | 0.43c |
| B700 | 76.10a | 1.07d | 5.32d | 0.36b | 17.15a | 0.17d | 0.05c | 10.45a | 2.54a | 0.32b | 0.06b | 0.00d | 7.88a | 0.37a | 0.18a | 0.55c |

EC[1]: electrical conductivity; WSOC[2]: water-soluble organic carbon; WSN[3]: water-soluble nitrogen; WSP[4]: water-soluble phosphorus.
The different lowercase letters in same column represent significant difference among the feedstock and biochars at $p < 0.05$ level.

## Assays

*Biochar*

Ten grams of biochar (< 0.25 mm) were thoroughly mixed with 100 mL of $CO_2$-free distilled water for 30 min. The pH value of the filtrate was determined with a UB-7 pH meter (Denver Instrument, Denver, USA). The electrical conductivity (EC) was measured with a conductivity meter (DDS-307, Shanghai Inesa Scientific Instrument Co. Ltd, Shanghai, China). The dissolved organic carbon (DOC), total nitrogen, phosphorus, $K^+$ and $Na^+$, and $Ca^{2+}$ and $Mg^{2+}$ were determined by the potassium dichromate volumetric method, Kjeldahl method, Mo-Sb colorimetric method, with a FP 640 flame photometer (Shanghai Inesa Scientific Instrument Co. Ltd, Shanghai, China), and with inductively coupled plasma spectrometry (ICP), respectively. The ash was analyzed by heating one gram of biochar sample at 500 °C for 4 h in a muffle furnace (Irfan *et al.* 2016). The contents of C, H, and N were estimated with an element analyzer (Vario EL III, Elementar, Frankfurt, Germany). The oxygen content was calculated as the difference between 100% and the sum of the C, H, N, and ash contents.

Portions of the biochar (10 g each) were thoroughly mixed with 100 mL of 1 mol/L HCl for 30 min in an oscillator (HY-5, Jiangsu) , and the biochar was then left overnight at room temperature in order to remove the minerals covered on biochar surface. The biochar was collected, washed with deionized water until the EC of the filtrate was less than 20 μS/cm, and dried at 105 °C. The surface area and pore distribution were determined by the mercury intrusion porosimetry method (Pore Master GT 60 aperture tester, Quantachrome, Boynton Beach, FL, USA), and the surface functional groups were determined with Fourier transform infrared spectroscopy (FTIR). The structure was observed with scanning electron microscopy (SEM).

Both the acidic and basic groups of the biochars were determined by the Boehm titration method. Portions of the acid-washed biochar (approximately 0.5 g each) were thoroughly mixed with 25.00 mL of 0.05 mol/L HCl, NaOH, or $NaHCO_3$ for 30 min, and then allowed to stand overnight. The filtrate of the HCl-added biochar was titrated with 0.05 mol/L NaOH. The basic group was calculated from the volume of NaOH solution that was consumed during titration. Both of the NaOH- and $NaHCO_3$-added biochar filtrates were titrated with 0.05 mol/L HCl. The acidic and carboxyl groups were estimated from the volume of HCl solution consumed during titration.

Portions of the HCl-washed biochar (approximately 0.2 g each) were thoroughly mixed with 20 mL of 1 mol/L sodium acetate (NaOAc) (pH 8.2) for 5 min, and then were centrifuged. The Na-saturated biochar was prepared by repeating the above process five times, and then washing the biochar with anhydrous alcohol five times. The adsorbed $Na^+$ was replaced by mixing the biochar with 1 mol/L ammonium acetate ($NH_4OAc$) (pH 7.0), and then centrifuging it five times. The Na-saturated biochar was then measured with a flame photometer. The CEC of the biochar was calculated from the replaced $Na^+$ quantity. The adsorption capacities of iodine and methylene blue were determined according to GB/T12496.8 (1999) and GB/T12496.10 (1999), respectively.

*Syngas*

The relative percentages of $CH_4$, $C_2H_6$, $C_2H_4$, $C_3H_8$, $C_2H_2$, $H_2$, CO, and $CO_2$ in the gas samples were analyzed by a gas chromatograph with A and B channels (PerkinElmer AutoSystem XL). Channel A was the PSS programmable inlet, which had a DB-5 capillary column (30-m length, 0.53-mm inner diameter, 0.25-μm

thickness), shunting rate of 30 mL/min, $N_2$ carrier gas flow rate of 3 mL/min, and hydrogen flame ionization detector (FID), and tested the organic gases. For the FID, the temperature was 250 °C. Channel B was the PKD packing column type inlet, which had a DB-5 capillary column (50-m length, 0.32-mm inner diameter, 1.00-μm thickness), helium carrier gas flow rate of 35 mL/min, and a thermal conductivity detector (TCD), and tested the inorganic gases. For the TCD, the temperature was 200 °C. The chromatographic column was maintained at 70 °C for 20 min.

*Bio-oil*

The high-temperature gaseous pyrolysis products were cooled with a shell-and-tube heat exchange condensing tube. The condensable bio-oil was stored under light-proof conditions at room temperature for several hours prior to assay. The water content was measured with a MA-1A automatic fast Karl Fischer water meter (Shanghai, China). The contents of C, H, O, and N in the non-aqueous fraction of bio-oil samples were determined with an EA3000 element analyzer (Leeman, Shanghai, China). The heating value in the non-aqueous fraction was estimated with an oxygen bomb calorimeter (Parr Instrument Co., Illinois, USA).

### Statistical Analysis

All data were expressed as the mean of three replicates on an oven-dried basis. The significant differences ($p < 0.05$) of the pyrolysis products prepared at different temperatures were compared using a one-way analysis of variance (ANOVA), and then expressed as the least significant difference ($LSD_{0.05}$) with the SAS software package (SAS 8.1).

## RESULTS AND DISCUSSION

### Yields of Bio-Products

The slow pyrolysis of switchgrass in a fixed-bed slow pyrolysis system at three temperatures produced 27.0% to 41.3% biochar, 26.3% to 40.9% syngas, and 30.8% to 34.1% bio-oil (Fig. 2). The biochar yield decreased with an increasing pyrolysis temperature, whereas the syngas yield increased and the bio-oil yield changed over a narrow range. It is supposed that the breaking of aliphatic bonds in holocellulose and lignin occurs at below 500 °C, whereas the rearrangement of the aromatic structures takes place at above 500 °C (Brebu and Vasile 2010; George *et al.* 2014; Volpe *et al.* 2017). Bio-products are greatly affected by both the lignocellulose content and pyrolysis temperature. Generally, a higher lignin content in the feedstock leads to a higher biochar yield (Cao *et al.* 2014). The slow pyrolysis of ligneous feedstock usually yields approximately 50% biochar, whereas holocellulosic feedstock yields 8% to 24% biochar. The switchgrass grown in saline soil contained 72.0% holocellulose and 10.0% lignin, which was much higher than those of the switchgrass grown in sweet soil (69.1%) (Zhao *et al.* 2017). Correspondingly, a higher biochar yield could be obtained compared with that of switchgrass grown in sweet soil (Imam and Capareda 2012). However, the biochar production fell within the range produced from cellulosic materials, such as corn straw (Chen *et al.* 2016). Moreover, a high pyrolysis temperature may have induced a further decomposition of the bio-oil and biochar, which reduced the yield of both, and increased the syngas production (Choudhury *et al.* 2014).

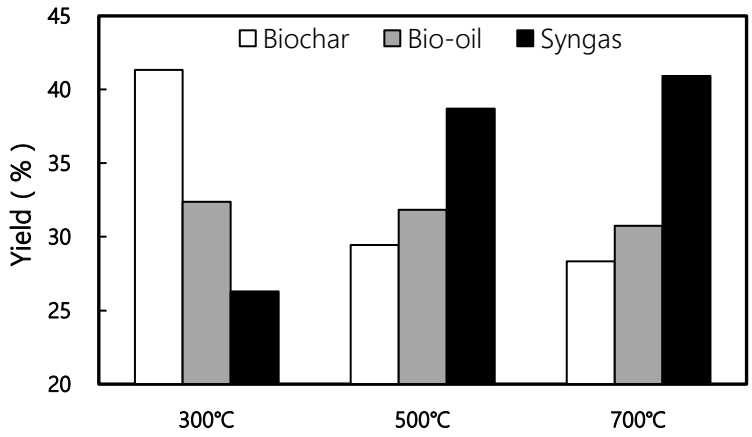


**Fig. 2.** Yields of the biochar, bio-oil, and syngas derived from switchgrass pyrolyzed at 300, 500, and 700 °C for 2 h in a fixed-bed pyrolysis system

## Bio-Oil

The water contents of the collected bio-oil ranged from 24.3% to 26.6%, and were not significantly affected by the temperature (Table 2). Bio-oil is composed of various condensable organic compounds, such as furfurals, phenols, polycyclic aromatic hydrocarbons (PAHs), and other minor compounds (Imam and Capareda 2012; Chen *et al.* 2016). The carbon content decreased with an increasing pyrolysis temperature, whereas the O and N contents increased, and the H content changed little with the increase of pyrolysis temperature. The heating value of the switchgrass bio-oil, which ranged from 17.99 to 22.11 MJ/kg, was as low as that from corn straw (19 to 23 MJ/kg). This might have been because of the high water content (Shah *et al.* 2012). The low C and high O contents also contributed to the low heating value of the bio-oil. It was obvious that the bio-oil derived from the switchgrass grown in saline soil with a fixed-bed slow pyrolysis reactor might be furtherly upgraded to obtain a higher-quality fuel though it had low value as a direct fuel.

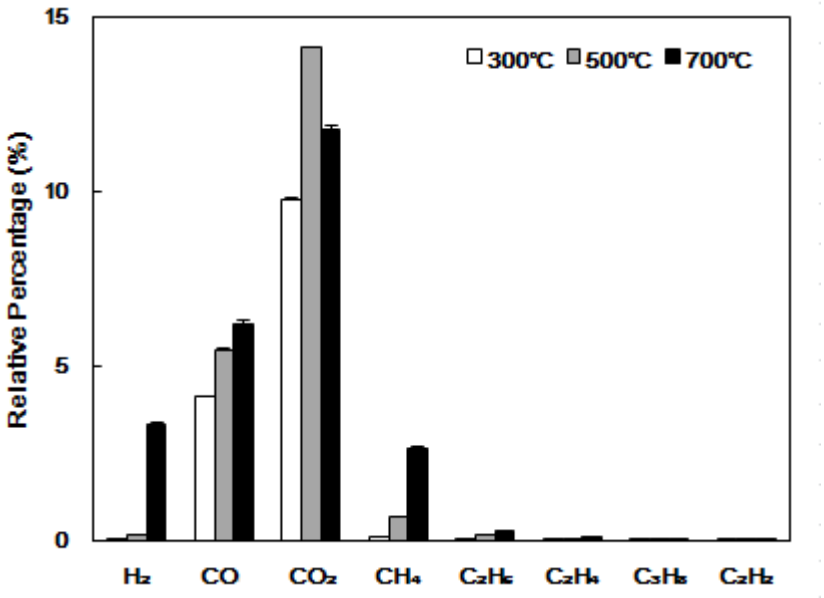


**Fig. 3.** Chemical composition of the syngas derived from switchgrass pyrolyzed at 300, 500, and 700 °C for 2 h in a fixed-bed pyrolysis system

**Table 2.** Water Content, Chemical Composition, and Heating Value of the Bio-Oil Derived from Switchgrass Pyrolyzed in a Fixed-Bed Pyrolysis System

| Bio-oil | Water Content | C | H | O | N | Heating Value |
|---|---|---|---|---|---|---|
| | % | | | | | MJ/kg |
| O300 | 26.60a | 54.88a | 7.13a | 37.33b | 0.66b | 22.11a |
| O500 | 24.27b | 52.79a | 6.38b | 39.85b | 0.98a | 19.87b |
| O700 | 26.39a | 45.51b | 7.54a | 45.95a | 1.00a | 17.99b |

The different lowercase letters in the same column represent significant differences among the feedstock and biochars at $p < 0.05$ level.

**Table 3.** Pore Structure Parameters of the Biochar Derived from Switchgrass Pyrolyzed in a Fixed-Bed Pyrolysis System

| Feedstock/biochars | Surface Area ($m^2/g$) | Specific Pore Volume ($cm^3/g$) | Mean Pore Diameter (μm) | Mode Pore Diameter (μm) | Median Pore Diameter (μm) |
|---|---|---|---|---|---|
| Feedstock | 5.67b | 1.72a | 1.21b | 14.55a | 12.70a |
| B300 | 2.40d | 1.05c | 1.73a | 3.09b | 3.02b |
| B500 | 7.44a | 0.98d | 0.53d | 1.49d | 1.52d |
| B700 | 4.09c | 1.16b | 1.14c | 2.03c | 1.83c |

The different lowercase letters in the same column represent significant differences among the feedstock and biochars at $p < 0.05$ level.

## Syngas

The major components of the harvested syngas were $CO_2$, CO, $CH_4$, and $H_2$, and combustible gases accounted for more than 30% of the total volume. The relative percentages of CO, $CH_4$ and $H_2$ increased with an increasing pyrolysis temperature (Fig. 3). The LHVs of the biogas were 4.04 to 8.66 MJ/Nm$^3$, which increased as the pyrolysis temperature increased. Syngas is believed to be derived from the decarboxylation, dehydrogenation, oxidation, and demethoxylation of biomass during pyrolysis (Brebu and Vasile 2010; Xiao *et al.* 2014). The retrogressive reactions of volatile compounds and solid products may also contribute to syngas production (Morgan and Kandiyoti 2014; Naqvi *et al.* 2014; Volpe *et al.* 2016). The lower LHV of the syngas derived from the switchgrass grown in saline soil, compared with that from switchgrass grown in sweet soil (11.8 to 20.0 MJ/Nm$^3$), may have been because of the high Na and K contents in the feedstock, which inhibited the formation of low-molecular hydrocarbons (Wang *et al.* 2007; Imam and Capareda 2012).

## Biochar

*General chemical properties of the biochar*

All of the values of the C content, pH, EC, ash, and water-soluble $K^+$ and $Na^+$ increased with an increasing pyrolysis temperature, whereas the H and O contents, water-soluble organic carbon (WSOC), water-soluble phosphorous (WSP), and water-soluble $Ca^{2+}$ decreased. Both water-soluble nitrogen (WSN) and water-soluble $Mg^{2+}$ were greatly reduced at 300 °C, but there was little change from 500 °C to 700 °C. It was obvious that the decomposition of the feedstock caused losses of H and O, and C enrichment. This resulted in a decrease in the atomic ratios of H/C and O/C, which ranged from 1.54 to 0.17, and from 0.70 to 0.05, respectively (Table 1). Generally, lower atomic ratios of H/C and O/C imply a higher carbonation degree, which corresponds with a higher biochar chemical stability. The ratios of both H/C and O/C in the biochar derived from switchgrass harvested from saline soil were lower than those from switchgrass grown in sweet soil, which might have been because of the different holocellulose and lignin contents in the two feedstocks (Conti *et al.* 2014; Aurangzaib *et al.* 2016). Therefore, the biochar derived from switchgrass grown in saline soil may have had a higher stability and be more suitable for use as a C sequestration material.

The pH and EC values of the biochar depend on the ash content and surface functional groups. Both decarboxylation and oxidation reduce acidic functional groups and increase basic functional groups, which may then enhance biochar alkalinity (Suliman *et al.* 2016). A high pyrolysis temperature usually induces a high ash content, pH, EC, and water-soluble mineral content (Rajkovich *et al.* 2012). It was evident that the much higher values of ash and pH in the biochar derived from switchgrass grown in saline soil compared with that from switchgrass grown in sweet soil was because of the high-soluble salts in the former (Conti *et al.* 2014). It was suggested that the biochar derived from the switchgrass grown in saline soil may have a remarkable liming effect and supply more mineral nutrients to plants if amended to soil (Dong *et al.* 2013; Xu *et al.* 2015).

*Pore structure*

The switchgrass feedstock had a complex surface structure and dominant pores that were 2 to 64 μm in diameter, which accounted for more than 80% of the total pore volume. Pyrolysis destroyed the feedstock surface structure, and it reduced the amount of

large pores, but it increased the amount of small pores (Fig. 4). The SEM images showed that the lignocellulosic structure broke up into small pieces, and the biochar surface became smooth (Fig. 5). The specific pore volume, mode pore diameter, and median pore diameter of the biochars decreased by 33% to 44%, 79% to 90%, and 76% to 88%, respectively, when compared with those of the feedstocks (Table 3). The surface area of the biochars reached a maximum of 7.44 $m^2/g$, which was 31% greater than that of the feedstock.

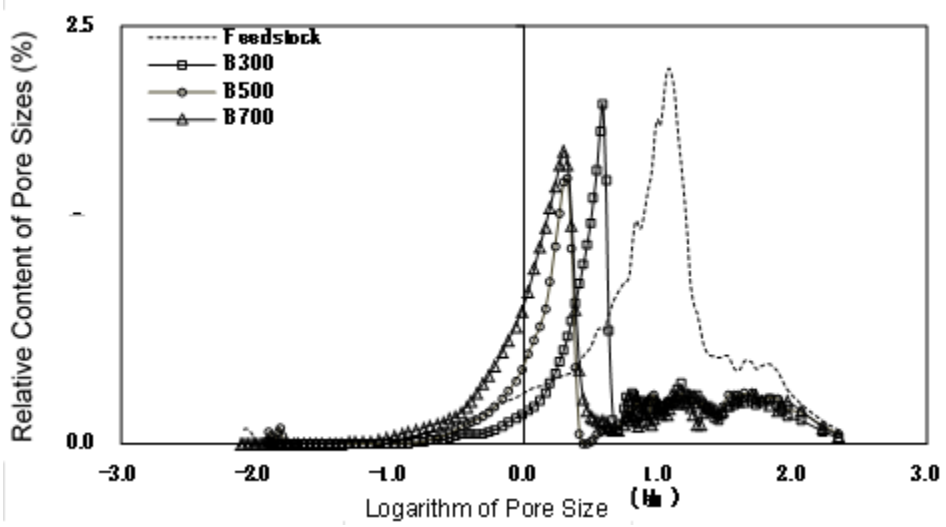


**Fig. 4.** Pore volume distribution of the biochar derived from switchgrass pyrolyzed at 300, 500, and 700 °C for 2 h in a fixed-bed pyrolysis system

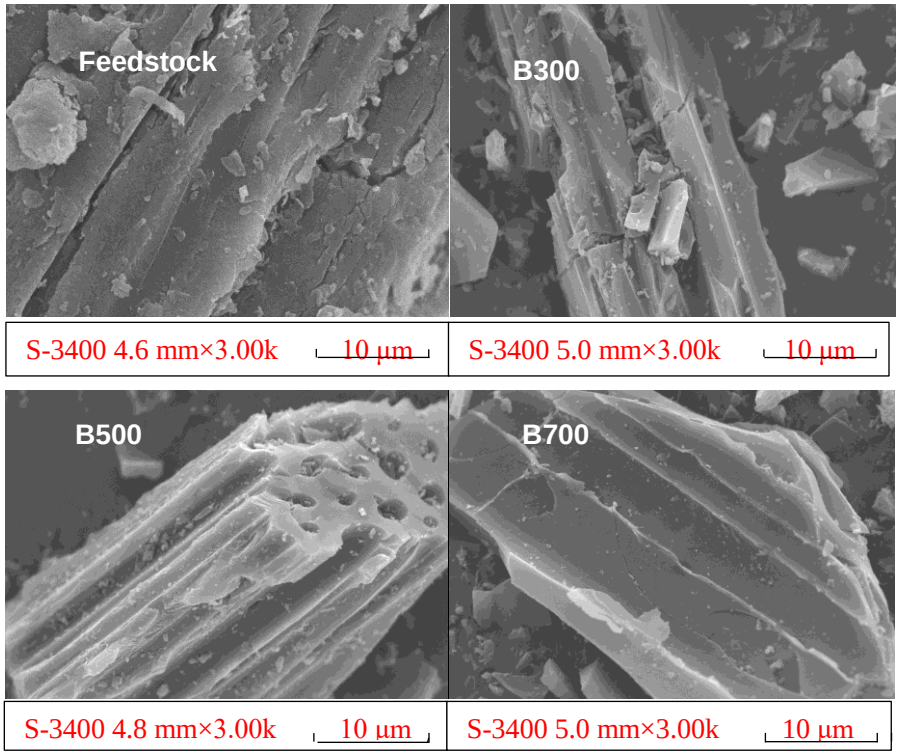


**Fig. 5.** SEM images of the feedstock and biochar derived from switchgrass pyrolyzed at 300, 500, and 700 °C for 2 h in a fixed-bed pyrolysis system

Low-temperature pyrolysis (< 200 °C) can lead to the evaporative loss of water and low-molecular compounds in the feedstock, and thus produce cavities that may form large pores. However, high temperature pyrolysis (> 300 °C) decreases large pores and increases small pores because of the synergic decomposition effect of hemicellulose, cellulose, and lignin (Tsai *et al.* 2012; Angın 2013; George *et al.* 2014). The pore structure changes in the switchgrass biochars were similar to those in other lignocellulosic biochars (Xiao *et al.* 2014). The biochar produced at 500 °C had a greater number of smaller pores and a larger surface area, which might enhance its performance as soil amendment and improve soil fertility (Alburquerque *et al.* 2014; Liu *et al.* 2016). Moreover, the small pores in the biochar may be conducive to bacterial and fungal colonization, and protect plants from being preyed on by soil fauna, such as protozoa (Warnock *et al.* 2007).

*Surface functional groups*

The FTIR spectra showed that the switchgrass feedstock had 14 peaks. The predominant functional groups were identified as -OH, $-CH_2$, C=O, aromatic C=C, aromatic rings, C-OH, and $-CH_3$. Pyrolysis significantly changed the amount and type of surface functional groups (Fig. 6).

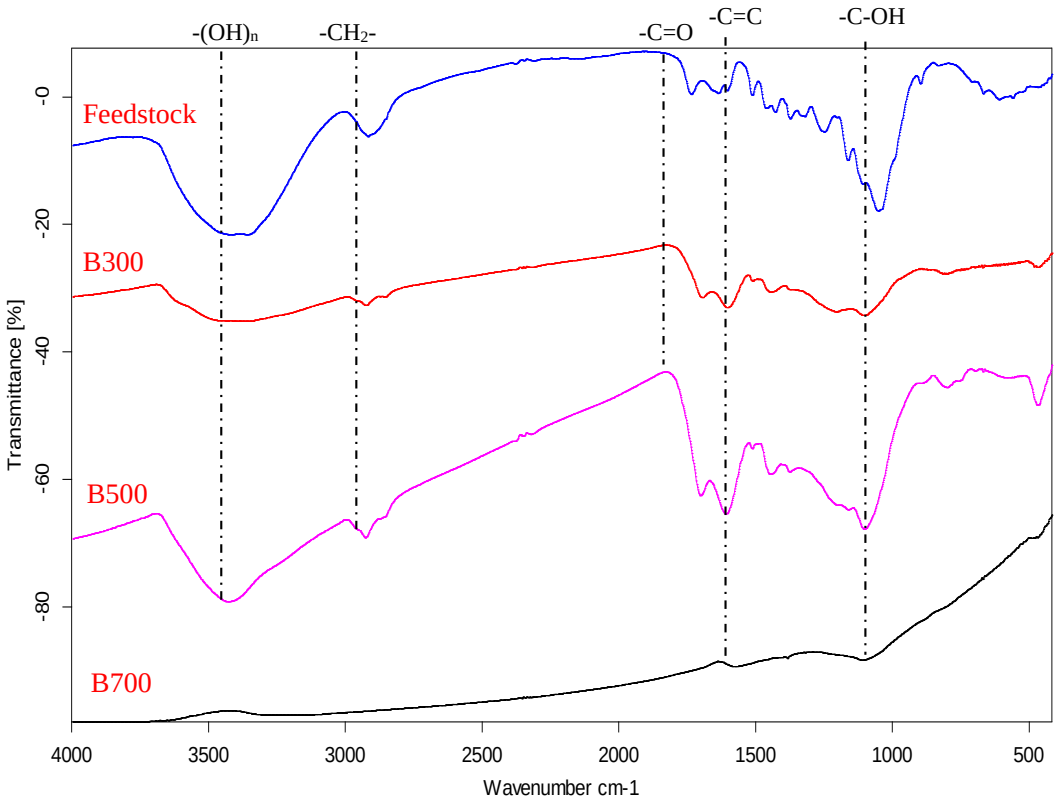


**Fig. 6.** FTIR spectra of the biochar derived from switchgrass pyrolyzed at 300, 500, and 700 °C for 2 h in a fixed-bed pyrolysis system

The B300 biochar had 9 peaks without $-CH_3$, which included the newly-formed functional groups of aromatic C=N (1605 $cm^{-1}$), nitroso N=O (1446 $cm^{-1}$), and S=O stretching vibration (1203 $cm^{-1}$). B500 and B700 had 7 and 2 peaks, respectively, which were primarily aromatic C=C and C-OH. Pyrolysis significantly increased the amount of basic functional groups from 0.11 mmol/g in the feedstock to 0.39 mmol/g in B700, but

significantly reduced the acidic functional groups content from 0.58 mmol/g in the feedstock to 0.14 mmol/g in B700. Carboxyl groups were predominant in the three biochars, which accounted for 32% to 64% of the total acidic functional groups, and the amount changed little above 500 °C (Fig. 7). McBeath *et al.* (2014) obtained similar results, and showed that biochars produced at high temperatures contained more aromatic groups and N-containing basic functional groups. Dehydrogenation, decarboxylation, and decarbonylation are considered to cause reductions in acidic functional groups, such as carbonyls and hydroxyls. The formation of aromatic functional groups, such as aromatic C=N, nitroso N=O, and aromatic C-OH, indicated a high chemical stability in the biochar, which may have a long residence time in soil and high potential for sequestering C (McBeath *et al.* 2014).

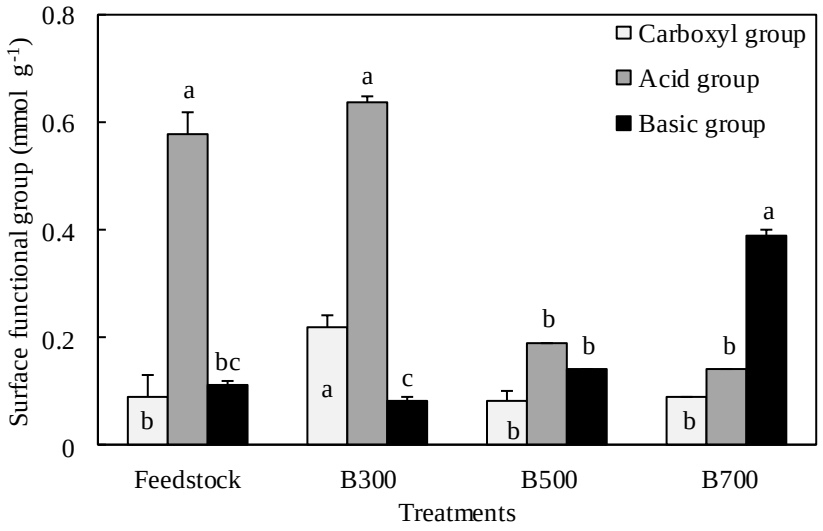


**Fig. 7.** Functional group concentrations of the biochar derived from switchgrass pyrolyzed at 300, 500, and 700 °C for 2 h in a fixed-bed pyrolysis system. The different lowercase letters represent significant difference at $p < 0.05$ in the same functional group among different treatments.

*Adsorption capacity*

Switchgrass feedstock can adsorb cations, nonpolar iodine, and polar methylene blue. Pyrolysis had no significant influence on the CEC, but it caused an average increase of 16% in iodine adsorption and an average reduction of 33% in methylene blue adsorption (Table 4). The CEC of the switchgrass biochar, which ranged from 200.3 to 241.1 cmol/kg, was significantly higher than that of biochar produced from lignocellulosic materials, such as corn straw and pine (15 to 80 cmol/kg). This implied that switchgrass biochar used as soil amendment would result in a remarkable improvement to the soil CEC, nutrient retention capacity, nutrient leaching, and nutrient use efficiency (Rajkovich *et al.* 2012). The iodine adsorption capacity of the switchgrass biochar, which ranged from 140.6 to 268.3 mg/g, was lower than that of bamboo shoot shell biochar (1038 to 1254 mg/g). This was because the pores that are greater than 1.0 nm, which is larger than the molecular size of iodine (0.6 nm), were predominant in the former (Ye *et al.* 2015). However, the obtained switchgrass biochars had higher methylene blue adsorption capacities, which ranged from 5.93 to 8.25 mg/g, compared with that of wheat straw biochar (< 4.5 mg/g). This may have been because of the pore

structure and surface polarity (Liu *et al.* 2012). The amphiphilic nature of biochar enables the adsorption of both nonpolar substances, such as iodine and benzene, and polar substances, such as methylene blue, atrazine, and pentachlorophenol, which shows their potential value in the removal of these pollutants (Xiao *et al.* 2014; Kuppusamy *et al.* 2016).

**Table 4**. CEC and Adsorption Capacity of the Biochar Derived from Switchgrass Pyrolyzed in a Fixed-Bed Pyrolysis System

| Feedsctok/biochars | CEC (cmol/kg) | Iodine Adsorption (mg/g) | Methylene Blue Adsorption (mg/g) |
|---|---|---|---|
| Feedstock | 218.02a | 193.82b | 10.44a |
| B300 | 212.95a | 265.77ab | 5.93c |
| B500 | 200.27a | 268.32a | 8.25b |
| B700 | 241.13a | 140.64c | 6.78bc |

The different lowercase letters in same column represent significant difference among the feedstocks and biochars at $p < 0.05$.

## CONCLUSIONS

1. The slow pyrolysis of switchgrass in a fixed-bed reactor at 300, 500, and 700 °C yielded 27% to 41% biochar and large volumes of syngas and bio-oil.
2. Both the syngas and bio-oil from a fixed-bed slow pyrolysis system might be upgraded through further process though low value as a direct fuel.
3. The biochar derived from the switchgrass grown in saline soil with a fixed-bed reactor had higher ash and mineral nutrient contents and CEC than that of the biochar from switchgrass grown in sweet soil. Meanwhile, that biochar pyrolyzed at 500 °C had high potential to be used as soil amendment.

## ACKNOWLEDGEMENTS

This study was supported by the National Natural Science Foundation of China (No. 41371243) and the National Key Technology R&D Program (No. 2013BAC02B06).

## REFERENCES CITED

Alburquerque, J. A., Calero, J. M., Barrón, V., Torrent, J., del Campillo, M. C., Gallardo, A., and Villar, R. (2014). "Effects of biochars produced from different feedstocks on soil properties and sunflower growth," *J. Plant Nutr. Soil Sci.* 177(1), 16-25. DOI: 10.1002/jpln.201200652

Angın, D. (2013). "Effect of pyrolysis temperature and heating rate on biochar obtained from pyrolysis of safflower seed press cake," *Bioresource Technol.* 128, 593-597. DOI: 10.1016/j.biortech.2012.10.150

Aurangzaib, M., Moore, K. J., Archontoulis, S. V., Heaton, E. A., Lenssen, A. W., and Fei, S. (2016). "Compositional differences among upland and lowland switchgrass

ecotypes grown as a bioenergy feedstock crop," *Biomass Bioenerg.* 87, 169-177. DOI: 10.1016/j.biombioe.2016.02.017

Biederman, L. A., and Harpole, W. S. (2013). "Biochar and its effects on plant productivity and nutrient cycling: A meta-analysis," *Glob. Change Biol. Bioenergy* 5(2), 202-214. DOI: 10.1111/gcbb.12037

Brebu, M., and Vasile, C. (2010). "Thermal degradation of lignin-A review," *Cellulose Chem. Technol.* 44 (9), 353-363.

Cao, X., Zhong, L., Peng, X., Sun, S., Li, S., Liu, S., and Sun, R. (2014). "Comparative study of the pyrolysis of lignocellulose and its major components: Characterization and overall distribution of their biochars and volatiles," *Bioresource Technol.* 155, 21-27. DOI: 10.1016/j.biortech.2013.12.006

Chen, M., Xu, P., Zeng, G., Yang, C., Huang, D., and Zhang, J. (2015). "Bioremediation of soils contaminated with polycyclic aromatic hydrocarbons, petroleum, pesticides, chlorophenols and heavy metals by composting: Applications, microbes and future research needs," *Biotechnol. Adv.* 33(6), 745-755. DOI: 10.1016/j.biotechadv.2015.05.003

Chen, T., Liu, R., and Scott, N. R. (2016). "Characterization of energy carriers obtained from the pyrolysis of white ash, switchgrass and corn stover — Biochar, syngas and bio-oil," *Fuel Process. Technol.* 142, 124-134. DOI: 10.106/j.fuproc.2015.09.034

Choudhury, N. D., Chutia, R. S., Bhaskar, T., and Kataki, R. (2014). "Pyrolysis of jute dust: Effect of reaction parameters and analysis of products," *Journal of Material Cycles and Waste Management* 16(3), 449-459. DOI: 10.1007/s10163-014-0268-4

Conti, R., Rombolà, A. G., Modelli, A., Torri, C., and Fabbri, D. (2014). "Evaluation of the thermal and environmental stability of switchgrass biochars by Py–GC–MS," *J. Anal. Appl. Pyrol.* 110, 239-247. DOI: 10.1016/j.jaap.2014.09.010

Dong, D., Yang, M., Wang, C., Wang, H., Li, Y., Luo, J., and Wu, W. (2013). "Responses of methane emissions and rice yield to applications of biochar and straw in a paddy field," *Journal of Soils and Sediments* 13(8), 1450-1460. DOI: 10.1007/s11368-013-0732-0

GB/T12496.8 (1999). "Test methods of wooden activated carbon - Determination of iodine number," Standardization Administration of China, Beijing, China.

GB/T12496.10 (1999). "Test methods of wooden activated carbon - Determination of methylene blue adsorption," Standardization Administration of China, Beijing, China.

George, A., Morgan, T. J., and Kandiyoti, R. (2014). "Pyrolytic reactions of lignin within naturally occurring plant matrices: Challenges in biomass pyrolysis modeling due to synergistic effects," *Energy Fuels* 28, 6918−6927. DOI: 10.1021/ef501459c

Huang, H. (2017). "Benefit analysis of strip intercropping between salt-tolerant forage and food crops," *China Agricultural University*, pp. 42-46.

Imam, T., and Capareda, S. (2012). "Characterization of bio-oil, syn-gas and bio-char from switchgrass pyrolysis at various temperatures," *J. Anal. Appl. Pyrol.* 93, 170-177. DOI: 10.1016/j.jaap.2011.11.010

Irfan, M., Chen, Q., Yue, Y., Pang, R., Lin, Q., Zhao, X., and Chen, H. (2016). "Co-production of biochar, bio-oil and syngas from halophyte grass (*Achnatherum splendens* L.) under three different pyrolysis temperatures," *Bioresource Technol.* 211, 457-463. DOI: 10.1016/j.biortech.2016.03.077

Jiang, Q., Webb, S. L., Yesudas, C. R., Bhandari, H. S., Narasimhamoorthy, B., Bouton, J. H., and Saha, M. C. (2014). "Variance components and heritability of biomass yield in switchgrass (*Panicum virgatum* L.) grown in the Southern Great Plains,"

*Field Crop. Res.* 168, 148-155. DOI: 10.1016/j.fcr.2014.07.016

Kan, T., Strezov, V., and Evans, T. J. (2016). "Lignocellulosic biomass pyrolysis: A review of product properties and effects of pyrolysis parameters," *Renew. Sust. Energ. Rev.* 57, 1126-1140. DOI: 10.1016/j.rser.2015.12.185

Kuppusamy, S., Thavamani, P., Megharaj, M., Venkateswarlu, K., and Naidu, R. (2016). "Agronomic and remedial benefits and risks of applying biochar to soil: Current knowledge and future research directions," *Environ. Int.* 87, 1-12. DOI: 10.1016/j.envint.2015.10.018

Liu, C., Wang, H., Tang, X., Guan, Z., Reid, B. J., Rajapaksha, A. U., Ok, Y. S., and Sun, H. (2016). "Biochar increased water holding capacity but accelerated organic carbon leaching from a sloping farmland soil in China," *Environ. Sci. Pollut. R.* 23(2), 995-1006. DOI: 10.1007/s11356-015-4885-9

Liu, Y., Zhao, X., Li, J., Ma, D., and Han, R. (2012). "Characterization of bio-char from pyrolysis of wheat straw and its evaluation on methylene blue adsorption," *Desalination and Water Treatment* 45(1-3), 115-123. DOI: 10.1080/19443994.2012.677408

Luo, Y. (2012). "The effect of miscanthus biochars on soil carbon and nitrogen transformation and its microbial mechanisms," *China Agricultural University*, pp. 87-90.

McBeath, A. V., Smernik, R. J., Krull, E. S., and Lehmann, J. (2014). "The influence of feedstock and production temperature on biochar carbon chemistry: A solid-state $^{13}C$ NMR study," *Biomass Bioenerg.* 60, 121-129. DOI: 10.1016/j.biombioe.2013.11.002

Mimmo, T., Panzacchi, P., Baratieri, M., Davies, C. A., and Tonon, G. (2014). "Effect of pyrolysis temperature on miscanthus (*Miscanthus* × *giganteus*) biochar physical, chemical and functional properties," *Biomass Bioenerg.* 62, 149-157. DOI: 10.1016/j.biombioe.2014.01.004

Morgan, T. J., and Kandiyoti, R. (2014). "Pyrolysis of coals and biomass: Analysis of thermal breakdown and its products," *Chem. Rev.* 114, 1547-1607. DOI: 10.1021/cr400194p

Naqvi, S. R., Uemura, Y., and Yusup, S. B. (2014). "Catalytic pyrolysis of paddy husk in a drop type pyrolyzer for bio-oil production: The role of temperature and catalyst," *J. Anal. Appl. Pyrol.* 106, 57-62. DOI: 10.1016/j.jaap.2013.12.009

Nelissen, V., Ruysschaert, G., Manka'Abusi, D., D'Hose, T., De Beuf, K., Al-Barri, B., Cornelis, W., and Boeckx, P. (2015). "Impact of a woody biochar on properties of a sandy loam soil and spring barley during a two-year field experiment," *Eur. J. Agron.* 62, 65-78. DOI: 10.1016/j.eja.2014.09.006

Rajkovich, S., Enders, A., Hanley, K., Hyland, C., Zimmerman, A. R., and Lehmann, J. (2012). "Corn growth and nitrogen nutrition after additions of biochars with varying properties to a temperate soil," *Biol. Fert. Soils* 48(3), 271-284. DOI: 10.1007/s00374-011-0624-7

Shah, A., Darr, M. J., Dalluge, D., Medic, D., Webster, K., and Brown, R. C. (2012). "Physicochemical properties of bio-oil and biochar produced by fast pyrolysis of stored single-pass corn stover and cobs," *Bioresource Technol.* 125, 348-352. DOI: 10.1016/j.biortech.2012.09.061

Suliman, W., Harsh, J. B., Abu-Lail, N. I., Fortuna, A., Dallmeyer, I., and Garcia-Perez, M. (2016). "Influence of feedstock source and pyrolysis temperature on biochar bulk and surface properties," *Biomass Bioenerg.* 84, 37-48. DOI: 10.1016/j.biombioe.2015.11.010

Tsai, W.-T., Liu, S.-C., Chen, H.-R., Chang, Y.-M., and Tsai, Y.-L. (2012). "Textural and chemical properties of swine-manure-derived biochar pertinent to its potential use as a soil amendment," *Chemosphere* 89(2), 198-203. DOI: 10.1016/j.chemosphere.2012.05.085

Volpe, R, Menendez, J. M. B., Reina, T. R., Messineo, A., Millan, M. (2017). "Evolution of chars during slow pyrolysis of citrus waste," *Fuel Process. Technol.* 158, 255-263. DOI: 10.1016/j.fuproc.2017.01.015

Volpe, R., Messineo, A., and Millan, M. (2016). "Carbon reactivity in biomass thermal breakdown," *Fuel* 183, 139-144. DOI: 10.1016/j.fuel.2016.06.044

Wang, S., Liu, Q., Liao, Y., Luo, Z., and Cen, K. (2007). "A study on the mechanism research on cellulose pyrolysis under catalysis of metallic salts," *Korean J. Chem. Eng.* 24(2), 336-340. DOI: 10.1007/s11814-007-5060-x

Warnock, D. D., Lehmann, J., Kuyper, T. W., and Rillig, M. C. (2007). "Mycorrhizal responses to biochar in soil – Concepts and mechanisms," *Plant Soil* 300(1), 9-20. DOI: 10.1007/s11104-007-9391-5

Xiao, L., Bi, E., Du, B., Zhao, X., and Xing, C. (2014). "Surface characterization of maize-straw-derived biochars and their sorption performance for MTBE and benzene," *Environmental Earth Sciences* 71(12), 5195-5205. DOI: 10.1007/s12665-013-2922-x

Xu, C.-Y., Bai, S. H., Hao, Y., Rachaputi, R. C. N., Xu, Z., and Wallace, H. M. (2015). "Peanut shell biochar improves soil properties and peanut kernel quality on a red Ferrosol," *Journal of Soils and Sediments* 15(11), 2220-2231. DOI: 10.1007/s11368-015-1242-z

Ye, L., Zhang, J., Zhao, J., Luo, Z., Tu, S., and Yin, Y. (2015). "Properties of biochar obtained from pyrolysis of bamboo shoot shell," *J. Anal. Appl. Pyrol.* 114, 172-178. DOI: 10.1016/j.jaap.2015.05.016

Yuan, H., Lu, T., Wang, Y., Chen, Y., and Lei, T. (2016). "Sewage sludge biochar: Nutrient composition and its effect on the leaching of soil nutrients," *Geoderma* 267, 17-23. DOI: 10.1016/j.geoderma.2015.12.020

Zhang, Y., Lin, F., Wang, X., Zou, J., and Liu, S. (2016). "Annual accounting of net greenhouse gas balance response to biochar addition in a coastal saline bioenergy cropping system in China," *Soil Till. Res.* 158, 39-48. DOI: 10.1016/j.still.2015.11.006

Zhao, X., Liu, J., Liu, J., Yang, F., Zhu, W., Yuan, X., Hu, Y., Cui, Z., Wang, X. (2017). "Effect of ensiling and silage additives on biogas production and microbial community dynamics during anaerobic digestion of switchgrass," *Bioresource Technol.* 241, 349-359. DOI: 10.1016/j.biortech.2017.03.183

Article submitted: April 18, 2017; Peer review completed: June 18, 2017; Revised version received: July 18, 2017; Published: July 24, 2017.
DOI: 10.15376/biores.12.3.6529-6544